Surface Functionalization of Thermoplastic Polymers for the Fabrication of Microfluidic Devices by Photoinitiated Grafting**

By *Thomas Rohr*, *D. Frank Ogletree*, *Frantisek Svec*, and *Jean M. J. Fréchet**

Photografting has been used for the surface modification of a wide range of commercial commodity polymers such as polystyrene, poly(methyl methacrylate), poly(dimethyl siloxane), polycarbonate, Parylene C, polypropylene, cyclic olefin copolymer, and hydrogenated polystyrene that are useful substrate materials for the fabrication of microfluidic chips. Since the chain propagation is initiated after UV light-activated abstraction of a hydrogen atom from the surface of channels within the materials, their permeability for UV light was tested and polyolefins were found to be the best candidates. A number of monomers with a variety of functional groups such as perfluorinated, hydrophobic, hydrophilic, reactive, acidic, basic, and zwitterionic have been successfully grafted from the surface of selected substrates, and the grafting efficiency determined using X-ray photoemission spectroscopy. Layered surface structures were prepared by consecutive grafting of different monomers. Our approach also enables photolithographic patterning of surfaces and specific functionalization of confined areas within the microchannel.

1. Introduction

The current rapid development of microfabricated analytical devices is fueled by the need of significant improvements in speed, sample throughput, cost, and handling of analyses. A variety of applications involving, for example, sensors, chemical synthesis, or biological analysis, have already been demonstrated using the microfluidic chip format. More complex micro total analysis systems (µTASs), the so-called "Lab-on-a-Chip", are expected to be implemented by combining a variety of functional building blocks within the chip.[1] Current approaches to µTAS largely rely on the use of inorganic substrates such as glass, silica, and quartz, in which the desired network of channels and other features are prepared using etching processes. The popularity of these materials stems from the ease of design and fabrication of prototypes as well as small series of microfluidic chips using the standard methods of microelectronics such as patterning and etching.[2]

However, the cost of the multistep wet fabrication of these microfluidic chips is high, and the use of thermoplastic polymer materials instead of hard inorganics would enable the use of inexpensive "dry" techniques such as injection molding or hot embossing. Consequently, there is growing interest in the development of polymeric substrates for the fabrication of microfluidic chips. Although an array of techniques is already available for the microfabrication of polymers incorporating microfluidic structures similar to those demonstrated in glass,[3,4] some practical issues such as the control of surface chemistry and the area available for surface interactions within microfluidic channels still remain to be addressed.

The chemistry of the surface of polymer-based devices is determined by the thermoplastic material used for their fabrication. For example, most of the commodity polymers available for this application are hydrophobic. These materials include, for example, polycarbonates (PC), poly(methyl methacrylate) (PMMA), polydimethylsiloxane (PDMS), poly(butylene terephthalate), and polyolefins such as polyethylene, polypropylene (PP), the copolymer of 2-norbornene ethylene ("cyclic olefin copolymer", COC), and hydrogenated polystyrene (PS-H). As a result of strong hydrophobic interactions, their surfaces can capture specific compounds from solution passing through the channels, changing their concentration in the solution, thus negating their precise quantitation. In addition, any molecules deposited on the wall of the channel also continuously change the character of the surface, further affecting both adsorption of other molecules and the reliability of quantitative assays. We believe that appropriate functionalization of the surface of the polymer microchannel would enable control of these undesired adsorption processes and greatly improve the reliability of polymer-based chips.

Standard open microchannels also suffer from a low surface-to-volume ratio. This is a serious problem in applications, such as chromatographic separations, heterogeneous catalysis, and solid-phase extraction, that largely rely on interactions with the solid surface. Since only the channel walls are used

[*] Prof. J. M. J. Fréchet,[+] Dr. T. Rohr, Dr. D. F. Ogletree, Dr. F. Svec[+]
E.O. Lawrence Berkeley National Laboratory
Materials Sciences Division
Berkeley, CA 94720 (USA)
E-mail: frechet@cchem.berkeley.edu

[+] Second address: Department of Chemistry, University of California, Berkeley, CA 94720-1460 (USA).

for the desired interaction, the open channel microdevices can only handle minute amounts of compounds. We have recently introduced monolithic porous polymer matrixes within the microchannels of glass microchips to achieve a considerable increase in their available surface areas.[5,6] Using the well-known primer silane reagent 3-(trimethoxysilyl)propyl methacrylate, the monoliths prepared in situ filled the channel cross section completely and were covalently attached to the glass surface via the primer silane moieties. Unfortunately, no such surface primer reagent is currently available for the treatment of polymer surfaces. Given the notoriously poor compatibility of most polymeric materials, it is likely that poor bonding of the monoliths to the walls of plastic chips will be observed, and that voids may even develop at the monolith–channel interface, thereby deteriorating significantly the performance of the devices. Therefore, the channel surface must be modified prior to the in-situ preparation of the monolith.

While the current literature presents countless examples of surface modifications of synthetic polymers, grafting is one of the most widespread techniques.[7] Although numerous grafting approaches have been demonstrated, most of them are not suitable for microfluidic chips, since grafting should only be performed in selected areas of the chips. This requirement disqualifies most of the approaches and favors processes triggered by UV light.

Photografting onto synthetic polymers was pioneered by Oster and Shibata in the late 1950s.[8] Later, Rånby developed rapid and efficient photografting techniques using benzophenone as a hydrogen-abstracting photoinitiator[9–14] and elucidated the mechanism of the process.[14] Since the grafted polymer chains may also contain abstractable hydrogen atoms, this type of graft polymerization creates branched and crosslinked architectures shown schematically in Figure 1. The wide range of both substrates[10,15–20] and monomers[10,15,16,18,20–28] amenable
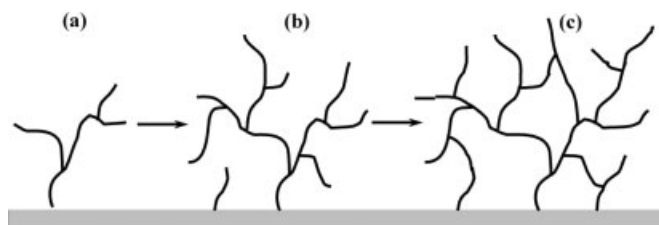

Fig. 1. Schematic representation of branched (a,b) and crosslinked (c) polymer architectures prepared using photografting initiated by benzophenone.

to photografting certainly makes this approach additionally attractive for the modification of microfluidic channels created in thermoplastic polymer devices. This report describes a simple and straightforward method for surface modification of commercial commodity polymers using UV-initiated photografting mediated by benzophenone, a process that proves to be well suited for the treatment of microfluidic devices. Using this method dramatic changes in the surface properties of the channels are demonstrated.

2. Results and Discussion

2.1. Chip Materials

In addition to material properties, such as melting point and melt viscosity, required for mass production using injection molding or embossing technologies, optical properties such as light transparency at the desired wavelength range and low background fluorescence are important characteristics of thermoplastic polymers that show potential for use in microfluidic chips.

The gray shaded area in Figure 2 represents the emission spectrum of the UV lamp used in this study. Since the photografting reactions must occur within the microchip channels surrounded on all sides by bulk polymer, the light must first
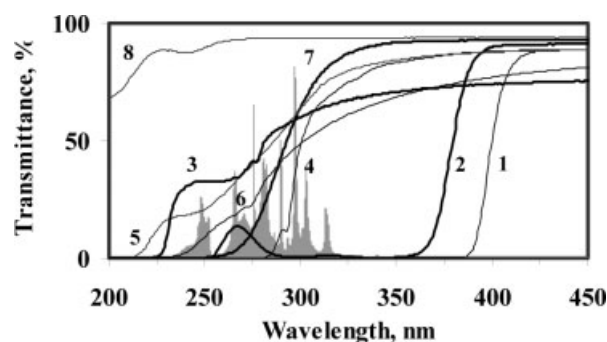

Fig. 2. Emission spectrum of the light source (gray) and UV-spectra of polycarbonate (1), poly(methyl methacrylate) (2), polydimethylsiloxane (3), polystyrene (4), cyclic olefin copolymer (5), hydrogenated polystyrene (6), Borofloat glass (7) and quartz (8).

pass through a layer of this polymer. Therefore, the materials must be transparent in a wavelength range of 230–330 nm. Figure 2 shows that quartz is transparent in the entire range, while PC is completely opaque and therefore not suitable for photografting. The other polymer materials tested all exhibit some transparency within this range of wavelength. Among the synthetic polymers, PDMS exhibits the best transparency in the far UV. However, its very low glass-transition temperature, T_g, makes this material suitable only for limited range of applications, such as rapid prototyping. PS-H, which has been developed for data storage and may be a future alternative to COC, is also sufficiently transparent and enables acceptable grafting. The UV transparency of COC, a commercially available engineering thermoplastic, is close to that of PDMS, and exceeds that of the glass. The same properties that make COC suitable for the manufacture of compact disks should make it useful for the reproduction of the fine relief features used in microfluidic devices. In addition, the chemical properties and solubility of COC are close to those of other members of the polyolefin family, including PE or PP. Therefore, COC dissolves only in solvents such as toluene and hexane that are less likely to be used in standard microfluidic applications. The desirable combination of mechanical, optical, and chemical properties makes COC currently one the best commercial candidate materials for the mass production of microfluidic chips, and therefore its use is broadly explored throughout this study.

The extent of optical transparency suggested by UV spectra shown in Figure 2 was confirmed by actual grafting experiments using the specifically designed chamber described in the Experimental section that simulates the microchip. A well-defined COC surface was obtained by spin coating its solution onto the surface of a silicon wafer. This coated wafer was placed in the test chamber, covered with an acrylamide solution (Table 1C), and irradiated. In order to closely mimic the grafting conditions found within the microchip, where the irra-

Table 1. Reaction conditions used for photografting.

Monomer mixture	Monomer [wt.-%]	BP [wt.-%]	Pluronic F-68 [wt.-%]	Solvent
A	bulk	3.0	–	–
B	30	0.67	0.67	H_2O
C	30	0.33	0.33	H_2O
D	15	0.33	0.33	H_2O
E	15	0.22	–	tBuOH-H_2O 3:1
F	15	0.22	–	tBuOH

diation of the internal channel always occurs through the bonded top cover, a sheet of a polymer was placed on top of the assembled mold.

Table 2 summarizes the results obtained after two minutes of grafting. Acrylamide was chosen since it contains nitrogen atoms, which are not present in COC and therefore useful in

Table 2. Photografting of acrylamide on COC using various polymers as a filter.

Filter	Irradiation power [mW/cm^2] [a]		2 min irradiation	
	260 [nm]	310 [nm]	N_{eff} [b]	Contact angle
Quartz	12.5	12.1	0.79	45
Borofloat glass	5.8	9.5	0.73	60
PS	2.1	5.6	0.62	61
PS-H	4.7	6.8	0.67	55
COC	7.9	9.6	0.79	48
PDMS	6.1	8.7	0.71	54
PMMA	0.4	0.1	0.39	60
PC	0	0	0 [c]	85 [c]

[a] Two probe heads (260 and 310 nm) cover the range between 220 nm and 340 nm shown in Figure 2. [b] Grafting efficiency calculated from atomic ratios determined by XPS (N/C found)/(N/C theoretical). [c] Irradiation time 30 min.
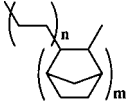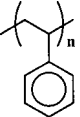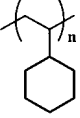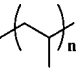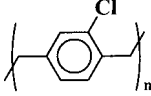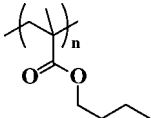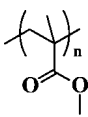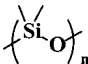
characterization. In addition, its grafting also changes the polarity of the original hydrophobic surface, enabling further measurements for the purpose of characterization. Grafting efficiency, N_{eff}, is obtained from X-ray photoemission spectroscopy (XPS) spectra by monitoring various atoms present in the surface and comparing observed and theoretical values. Since COC coated on the silicon wafers is a pure hydrocarbon, it only affords an XPS signal for carbon. Therefore, both the N/C ratio and consequently N_{eff} are equal to zero for the original COC layer. Since the grafting of polyacrylamide onto COC results in the incorporation of nitrogen atoms, the N/C ratio increases, and so does N_{eff}. If the thickness of the grafted polymer layer exceeds the depth that can be examined by XPS (~ 10 nm), no further change in atomic ratios can be observed, and the efficiency reaches the maximum value of one. In practice, quantitation via XPS is limited by the atomic sensitivity factors. These

are determined using bulk inorganic compounds[29] to estimate the relative response for different elements. Since the propagation of the XPS electrons through the polymer is slightly different than through the reference materials, there remains an uncertainty of up to 15–20 % in the calibration due to matrix effects. This uncertainty is found in the calibration, but not in the measurement itself. It must be emphasized that the value of N_{eff} is not the yield of the grafting reaction, but rather a measure of its success.

The results in Table 2 clearly confirm the opacity of PC, since no transmitted light was detected using this material as a filter, and no grafting was achieved even after 30 min of irradiation. However, transmittance of UV light and photografting were observed for all other materials. The grafting efficiency values correlate well with the irradiation power for both probe heads and with the measured values of contact angles. Although COC is the most transparent of the polymers tested, its transmission is significantly lower than that of quartz. Despite this finding, a similar extent of grafting was measured after irradiation through both quartz and COC. This can be explained by the formation of polymer layers that exceed the depth of analysis provided by XPS. Indeed, grafting times extended from two to five minutes did not result in any significant increase in the measured value of N_{eff}. The similarity of grafting obtained by irradiation through Borofloat glass, PS, and PDMS—all materials with very different optical properties—indicates that efficient photografting takes place within a broad range of wavelengths from 230 to 320 nm. The lowest grafting efficiency was observed for PMMA, which has only a small transmission window at 260 nm. In this case, grafting is accompanied by depolymerization and formation of a layer of degradation products soluble in methanol at the outer surface of the PMMA sheet when irradiation times exceeded three minutes. After treatment with methanol, the surface appears hazy or white.

Since most of the polymers mentioned above are potentially useful for the fabrication of microfluidic chips, their modification using grafting constitutes a suitable technique for the control of their surface properties. For our tests, COC, PS, as well as PBuMA were spin coated, while Parylene C was vapor deposited on silicon wafers. Flat sheets of PMMA, PS-H, and PDMS were used directly, and PP films were prepared by melting small pieces of this polymer between two glass slides. These samples were placed in the polymerization chamber, and the top quartz window was not covered with any polymer for these experiments. All the grafting experiments were done using acrylamide to enable monitoring of nitrogen atoms by XPS. Table 3 shows the contact angles prior to and after grafting, as well as the grafting efficiencies. With an irradiation time of five minutes, grafting occurred for all substrates containing easily abstractable methylene or methine hydrogen atoms. Best results were obtained with COC, while PDMS having only methyl groups reacted slowly with 30 min of irradiation needed to achieve the desired grafting efficiency. Good results were also obtained for grafting onto PBuMA, and this finding forms the basis of an ongoing study of the surface modification of porous materials, which will be published elsewhere.

Table 3. Photografting of various polymers with acrylamide. [a]

Polymer	Structure	Contact angle		N_{eff} [b]
		original	grafted	
COC		89	46	0.89
PS		90	52	0.71
PS-H		89	47	0.82
PP		91	46	0.85
Parylene C		86	47	0.68
PBuMA		78	50	0.63
PMMA		66	53	0.62
PDMS [c]		98	68	0.49

[a] Monomer mixture C, irradiation time 5 min. For other conditions see Experimental. [b] Grafting efficiency as the ratio (N/C found)/(N/C theoretical). [c] Irradiation time 30 min.

2.2. Grafting of Various Monomers

Since a variety of different chemistries might be required in microfluidic devices, we have optimized the grafting conditions for a large number of monomers including perfluorinated, hydrophobic, hydrophilic, reactive, acidic, basic, and zwitterionic species with a broad range of properties. Table 4 shows the grafting efficiencies calculated from XPS data using the atomic ratios of the heteroatoms oxygen, nitrogen, sulfur, and fluorine that would be typical of the various monomers.

Most of the monomers graft well onto COC substrate; generally, acrylates are superior to methacrylates, for which the hydrogen abstraction occurs also from the methyl group of the methacryloyl moiety producing a less reactive allylic radical.[18]

In addition, the polymethacrylate backbone only contains quaternary carbons and methylene groups from which only the hydrogen atoms can be abstracted, whereas polyacrylate chains contain both methylene and more reactive methine hydrogens that both facilitate grafting and the formation of highly branched structures.

Some of the grafting efficiencies shown in Table 4 exceed the highest theoretical value of one. This can be assigned to the overall calibration error inherent to of XPS (vide supra). However, the validity of our XPS measurements is confirmed by the 1:1 ratio between the carbon atoms bound to oxygen ($>C=O$ and $-O-C-$) that is always observed in the high-resolution XPS spectra of carbon for both grafted aliphatic acrylates and methacrylates. Similar measurements with grafted fluorinated monomer 2,2,3,3,4,4,4-heptafluorobutyl acrylate (HFBA) afford ratios of 2.1:1.0:1.0:1.9:1.1 for the carbon atoms of the repeat unit of the main chain, $>C=O$, $-O-C-$, $>CF_2$, and $-CF_3$, which are close to the theoretical values of 2:1:1:2:1.

2.3. Effect of Channel Depth

Obviously, even a thickness of only a few micrometers of a UV-absorbing material or solution would decrease the intensity of the UV light and, consequently, the grafting efficiency.[18] The depth of features in typical microfluidic chips may reach several tens of micrometers. To better mimic this reality in our initial experiments, we used 50 µm thick layers of the monomer solutions through the use of appropriate PE gaskets in the polymerization chamber. However, it was important to assess the effect of UV transparency of the polymerization mixtures during the grafting more precisely in order to determine the depth of the channel through which sufficient grafting can be safely achieved.

Figure 3 shows the contact angles and grafting efficiencies for COC after irradiation through either bulk methyl acrylate (MA, Procedure A of Table 1) or an aqueous solution of 2-acrylamido-2-methyl-1-propanesulfonic acid (AMPS, Procedure B of Table 1) for five minutes in a chamber fitted with several PE gaskets having thicknesses of 25, 50, 100, and 200 µm. The self-screening effect of MA is significant, as the grafting efficiency decreases from 84 % for the lowest layer thickness to 31 % for a layer 200 µm thick. The measured contact angles correlate well with this finding. Most encouraging is the fact that some grafting is possible in the presence of 3 wt.-% of benzophenone, even through a 200 µm layer of the bulk MA.

During these experiments, we also observed an increase in viscosity of the liquid that indicated the concomitant formation of a considerable amount of homopolymer in the solution. The extent of this homopolymerization can be reduced by diluting the monomer with a suitable solvent. Dilution with a solvent that has lower absorbance in the UV range than the monomer itself also helps to reduce the negative self-screening effect of the monomer. This is confirmed by the considerably smaller effect of layer thickness observed during the grafting process carried out with a 30 wt.-% aqueous solution AMPS. The grafting

Table 4. Photografting of COC with various monomers.

Monomer	Conditions/ Extraction	Irrad [a]	Structure	R	Grafting efficiency [b]			
					O	N	S	F
MA	A / acetone	5		H	0.86	–	–	–
MMA	A / acetone	5		CH₃	0.55	–	–	–
BuA	A / acetone	5		H	1.05	–	–	–
BuMA	A / acetone	5		CH₃	0.61	–	–	–
tBuA	A / acetone	5		H	1.23	–	–	–
tBuMA	A / acetone	5		CH₃	0.86	–	–	–
HEA	B / H₂O	0.5		H	0.47	–	–	–
HEMA	B / H₂O	5		CH₃	0.93	–	–	–
AAc	B / H₂O	5		H	0.86	–	–	–
MAAc	B [c]/ H₂O	5		CH₃	0.86	–	–	–
GMA	A / acetone	5		–	0.26	–	–	–
EDA	A / acetone	0.5		H	0.92			
EDMA	A / acetone	0.5		CH₃	0.16			
		2		CH₃	0.68			
AAm	C / H₂O	5		–	0.72	0.90	–	–
NIPAAm	D [c] / H₂O	5		CH₃	0.99	0.87	–	–
	E / H₂O	5		CH₃	0.97	0.91	–	–
NEAAm	E / H₂O	5		H	0.62	0.52	–	–
SPA	D [c] / H₂O	5		H	0.83	–	0.56	–
SPM	D [c] / H₂O	5		CH₃	0.77	–	0.45	–
AMPS	B [c] / H₂O	5		–	0.63	0.62	0.39	–
	E / H₂O	5		–	0.75	0.81	0.48	–
AGA	D [c] / H₂O	5		–	0.80	0.80	–	–
SPE	D [c] / H₂O	5		–	0.87	0.62	0.59	–
META	B [c] / H₂O	5		–	0.63	0.52	–	–
DPMA	A / acetone	5		–	0.17	0.11	–	–
	B [c]/acetone	5		–	0.58	0.48	–	–
VAL	A / acetone	5		–	0.22	0.16	–	–
	F / acetone	5		–	0.40	0.39	–	–
HFBA	A / HFP	5		–	1.06	–	–	1.21
PFOA	A / HFP	5		–	1.16	–	–	1.33
PFPA	A / HFP	5		–	0.33	–	–	0.32

[a] Irradiation time [min]. [b] Calculated for each element as the ratio (X/C found)/(X/C theoretical) for X = O, N, S, or F. [c] Remains emulsion.

efficiency based on XPS monitoring of the abundance of sulfur (Fig. 3) shows only a moderate decrease from 0.66 to 0.48 upon increasing the cell thickness from 0 to 200 μm.

2.4. Grafting of Copolymers

Copolymerization of two or more monomers can be used to fine tune the surface properties. The percentage of each monomer incorporated in the polymer chains depends on their reactivity ratios and the composition of the polymerization mixture. Since the overall amount of grafted copolymer is small, both the composition of the monomer mixture and the composition of the formed polymer chains do not change significantly during the grafting process. Model grafting experiments with spin-coated COC were performed using a mixture of hydrophobic butyl acrylate (BuA) and ionizable AMPS (Table 1E) with an irradiation time of five minutes. Since AMPS also contains sulfur, its incorporation in the copolymers is readily estimated from XPS spectra using the S/C or S/O atomic ratios. Although use of S/C ratios for the calculations is simpler, this can be affected by the significant carbon signal of the COC support layer. Therefore, we used the S/O ratio, taking into consideration the oxygen content in both AMPS and BuA. Table 5 summarizes the results of copolymerizations obtained upon varying the composition of the monomer mixture. The reactivity ratios of AMPS and BuA are very different, and the composition of the copolymer deviates significantly from the proportion of monomers in the polymerization mixture. The relationship between the AMPS fraction in monomer mixture f_{AMPS} and in copolymer F_{AMPS} shown in Table 5 matches that found for similar copolymerizations in solution.

2.5. Grafting of Layers

The photografting process presented in this study does not allow the formation of linear block architectures. However, using a sequence of photografting reactions, several layers can be polymerized on top of each other. This approach has been demonstrated by the sequential photografting of acrylic acid and *N*-isopropylacrylamide (NIPAAm) onto polyethylene films.[25] We assumed that this
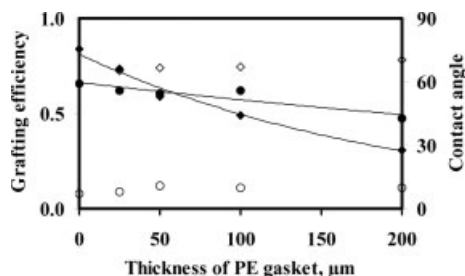
Fig. 3. Effect of seal thickness on grafting efficiency calculated from abundance of oxygen for methyl acrylate (1, ◆) and sulfur for 2-acryamido-2-methylpropanesulfonic acid (2, ●) and contact angles of the two grafted surfaces (◇) and (○), respectively. The point at 0 μm was obtained using an assembly slightly different from that described in the Experimental. The mold consisted of a plain silicon wafer, a 50 μm PE gasket, a spin-coated quartz microscope cover glass (200 μm thick) positioned upside-down, and the 1.6 mm quartz wafer cover. The light did not pass through the solution.

Table 5. Preparation of photografted AMPS and nBuA copolymers.

f_{AMPS} [a] [wt.-%]	f_{AMPS} [a] [mol-%]	S/C	S/O	F_{AMPS} [b] (S/C)	F_{AMPS} [b] (S/O)
1.00	1.00	0.084	0.17	1.00	1.00
0.85	0.93	0.064	0.15	0.76	0.78
0.74	0.82	0.042	0.12	0.50	0.51
0.50	0.62	0.015	0.06	0.18	0.21
0.20	0.29	0.003	0.01	0.03	0.05
0.04	0.06	0.00	0.00	0.00	0.00
0.00	0.00	0.00	0.00	0.00	0.00

[a] Fraction of AMPS in monomer mixture. [b] Fraction of AMPS in the grafted copolymer calculated from experimental S/C and S/O ratios obtained using XPS.

approach would also enable the generation of polymer shells and shielding of functionalities "hidden" in the lower layer preventing their interactions with specific compounds in an analyte solution. For example, the sulfonic acid groups of AMPS are required to generate electro-osmotic flow. However, they can also absorb peptides and proteins via Coulombic interactions. Thus, steric shielding similar to that typical of restricted-access media for HPLC[30,31] can be achieved by covering the grafted AMPS layer with another layer of polymer with desired properties. Thus, grafting in layers may be particularly useful for the preparation of microfluidic electrochromatographic devices.

The proof of this concept is demonstrated in Figure 4 on a four-layer system. Alternating layers of AMPS (A) and BuA (B) (Table 1E) were photografted for five minutes on spin-coated COC. Since the thickness of the grafted polymer layers is less than the sampling depth of XPS, sulfur is detected in each layer. However, its content is significantly higher when
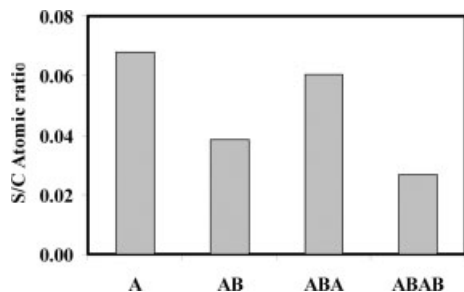

Fig. 4. S/C atomic ratio for subsequently grafted "block-like" layers using 2-acryamido-2-methylpropanesulfonic acid (A) and butyl acrylate (B).

polyAMPS forms the top layer (Fig. 4, A and ABA). Swelling of the previously prepared polymer layer in the subsequent monomer mixture also contributes to a decreased sharpness of the boundary at the interface of the two polymer layers.

2.6. Patterning

Photografting triggered by UV light through a mask facilitates patterning. This is a major advantage of this method compared to both thermally and redox-initiated grafting techniques. The qualitative effect of the intensity of the UV light on the grafting efficiency was presented above for experiments in which different polymers were used as filters to modulate intensity. The use of a photomask such as a multi-density resolution target (Series I, Ditric Optics, Hudson, MA) that includes several fields differing in UV light transmittance enables quantitative evaluation. Figure 5 illustrates the effect of irradiation through this step-gradient mask on the grafting efficiency of
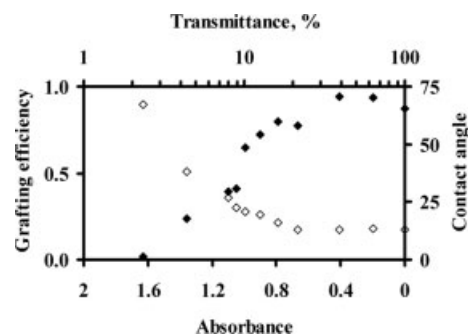

Fig. 5. Grafting efficiency determined from S/C ratio (1, ◆) and contact angle (2, ◇) for 2-acryamido-2-methylpropanesulfonic acid grafted for 5 min using irradiation through a multi density target.

AMPS and the contact angle of the surface (Table 1E, 5 min irradiation). The absorbance values of the fields of the multi-density target varied between 0.2–1.6. The values obtained for each field were normalized with respect to the grafting in systems containing only a quartz plate with an absorbance value of zero. As expected, the grafting efficiency increases linearly with decreasing absorbance, until it reaches the point at which the grafted layer thickness exceeds the depth of information of XPS, where it levels out. The contact-angle values confirm the trends obtained for the grafting efficiencies. The higher the extent of the grafting, the lower the contact angle. Grafting through masks with a gradient of absorbance enables the fabrication of layers with both stepwise and continuous gradients of hydrophilicity, polarity, acidity, or combinations thereof along the channel by simply using multi-density, continuous grayscale photomasks or a moving shutter.

3. Conclusion

UV-initiated photografting within the channels of a microfluidic device is a simple and versatile approach that enables the

FULL PAPER

surface modification of synthetic polymers with a wide variety of chemistries and at precisely defined locations in an easy single step. We expect that this approach will facilitate the design and preparation of numerous new functional elements that are instrumental to the development of complex microanalytical systems. In contrast to the present state-of-the-art glass chips that are produced using the typical microfabrication techniques developed for microelectronics, thermoplastic materials are more suitable for mass production using technologies such as injection molding and hot embossing. Our approach opens new avenues that may help in the development of low-cost functional microdevices and systems for a variety of specific applications.

4. Experimental

Materials: Methyl acrylate (99 %, MA), methyl methacrylate (99 %, MMA), butyl acrylate (99 %, MA), butyl methacrylate (99 %, BuMA), *tert*-butyl acrylate (98 %, *t*BuA), *tert*-butyl methacrylate (98 %, *t*BuMA), 2-hydroxyethyl acrylate (96 %, HEA), 2-hydroxyethyl methacrylate (98 %, HEMA), acrylic acid (99 %, AAc), methacrylic acid (99 %, MAAc), glycidyl methacrylate (97 %, GMA), ethylene diacrylate (90 %, EDA), ethylene dimethacrylate (98 %, EDMA), acrylamide (99 %, AAm), *N*-isopropylacrylamide (97 %, NIPAAm), 3-sulfopropyl acrylate, potassium salt (SPA), 2-acrylamido-2-methyl-1-propanesulfonic acid (99 %, AMPS), 2-acrylamidoglycolic acid monohydrate (96 %, AGA), [2-(methacryloyloxy)ethyl]-trimethylammonium chloride (75 wt.-% solution in water, META), *N*-[3-(dimethylamino)propyl]methacrylamide (99 %, DPMA), benzophenone (99 %, BP), 1-dodecanol (98 %), cyclohexanol (99 %), 1,1,1,3,3,3-hexafluoro-2-propanol (99 %, HFP), and 2,2-dimethoxy-2-phenylacetophenone (99 %, DAP) were purchased from Aldrich. *N*-Ethylacrylamide (NEAAm) was obtained from Monomer-Polymer & Dajac Laboratories (Feasterville, PA). Pentafluorophenyl acrylate (PFPA) was obtained from Polysciences (Warrington, WA) and 2,2,3,3,4,4,4-heptafluorobutyl acrylate (97 %) and 1H,1H-perfluorooctyl acrylate (97 %, PFOA) from Lancaster Synthesis (Windham, NH). 3-Sulfopropyl methacrylate, potassium salt (SPM) was a gift from Raschig, (Richmond, VA), and [2-(methacryloyloxy)ethyl]dimethyl(3-sulfopropyl)ammonium hydroxide, inner salt (SPE) and 4,4-dimethyl-2-vinylazlactone (VAL) were gifts from 3M Company (St. Paul, MN). Pluronic F-68 was purchased from Sigma, St. Louis, MO.

Poly(butyl methacrylate) (PBuMA) was synthesized from BuMA using a standard free-radical procedure. Polystyrene (PS), poly(methyl methacrylate) (PMMA), and poly(dimethyl siloxane) (PDMS) were standard-grade sheet materials, the Parylene C layer was prepared by vapor deposition onto standard silicon wafers. Cyclic olefin copolymer (Topas 8007 X-10, COC) and hydrogenated polystyrene (PS-H) were obtained as gifts from Ticona (Summit, NJ) and Bayer AG (Leverkusen, Germany), respectively.

VAL was distilled prior use. MA, MMA, BuA, BuMA, tBuA, tBuMA, HEA, HEMA, EDA, and EDMA were purified by passing them through a bed of basic alumina (Brockman activity I, 60-325 mesh) to remove inhibitors, and distilled under reduced pressure. All other monomers were used as received.

Light Source: An Oriel deep-UV illumination system series 8700 (Stratford, CT) fitted with a 500 W HgXe lamp was used for UV exposure. The irradiation power was calibrated to 15.0 mW cm^{-2} using an OAI Model 354 exposure monitor (Milpitas, CA) with a 260 nm probe head. The emission spectrum of the exposed light was recorded using a UV–Raman spectrometer [32].

Characterization Methods: UV-transmission spectra were recorded using a Varian Cary 50 Conc UV-vis spectrometer (Lexington, MA). Contact-angle measurements were performed using a Krüss contact angle measuring system G10 (Charlotte, NC). Contact angles were taken in the static mode, 2 min after the application of the droplet. X-ray photoemission spectroscopy (XPS) was performed with a Physical Electronics PHI 5400 ESCA, equipped with an Omni II small-spot lens, using an Al anode X-ray source.

Spin Coating: A filtered 10 wt.-% solution of polymers in toluene (COC and PS) or acetone (PBuMA) was applied to silicon wafers (50 mm × 0.3 mm, Pure Sil, Bradford, PA), spin coated at 3000 rpm for 40 s, and dried overnight at room temperature. The wafers were cut to four equal wedges prior to their grafting.

Monomer Mixtures for Photografting: The compositions of the monomer mixtures used for grafting are summarized in Table 1. The surfactant Pluronic F-68 was added to aqueous systems to improve the solubility of benzophenone. All mixtures were de-oxygenated by purging with nitrogen for 10 min prior to photografting.

Photografting: Spin-coated silicon wafers or sheets of polymers were placed on the top of an aluminum base. A PE gasket (50 μm thick, unless otherwise stated) was prepared to frame the flat sample, and a small channel was cut into the gasket at one corner. A 1.6 mm thick and 100 mm diameter quartz wafer containing a 1 mm hole was placed on the top of the gasket with the hole located at the side opposite to the channel in the gasket. This assembly was sandwiched between an aluminum ring and the base and fixed with four screws. The purged monomer solution was injected through the hole in the quartz wafer, and the void between the polymer surface and the quartz wafer defined by the gasket was filled with monomer solution via capillary action. A black tape mask was attached to the top of the quartz window exactly over the PE gasket to avoid photolamination between the base polymer and the gasket. The tape also covered the hole used for filling. Additional filters or photomasks were then placed on the top of this assembly. Illumination with UV light was carried out from a distance of 30 cm for specific periods of time. The grafted samples were carefully removed, washed first with a suitable solvent, followed by extraction in this solvent for another 12 h to remove soluble polymer, and dried in a vacuum oven at room temperature for 24 h.

[1] A. van den Berg, T. S. J. Lammerink, *Top. Curr. Chem.* **1998**, *194*, 21.
[2] D. Qin, Y. N. Xia, J. A. Rogers, R. J. Jackman, X. M. Zhao, G. M. Whitesides, *Top. Curr. Chem.* **1998**, *194*, 1.
[3] H. Becker, C. Gartner, *Electrophoresis* **2000**, *21*, 12.
[4] J. Rossier, F. Reymond, P. M. Michel, *Electrophoresis* **2002**, *23*, 858.
[5] T. Rohr, C. Yu, M. H. Davey, F. Svec, J. M. J. Fréchet, *Electrophoresis* **2001**, *22*, 3959.
[6] C. Yu, M. H. Davey, F. Svec, J. M. J. Fréchet, *Anal. Chem.* **2001**, *73*, 5088.
[7] Y. Uyama, K. Kato, Y. Ikada, *Adv. Polym. Sci.* **1998**, *137*, 1.
[8] G. Oster, O. Shibata, *J. Polym. Sci.* **1957**, *26*, 233.
[9] W. T. Yang, B. Rånby, *J. Appl. Polym. Sci.* **1996**, *62*, 533.
[10] B. Rånby, *Mater. Res. Innovations* **1998**, *2*, 64.
[11] B. Rånby, *Makromol. Chem., Macromol. Symp.* **1992**, *63*, 55.
[12] B. Rånby, *Int. J. Adhes. Adhes.* **1999**, *19*, 337.
[13] W. T. Yang, B. Rånby, *Polym. Bull.* **1996**, *37*, 89.
[14] B. Rånby, W. T. Yang, O. Tretinnikov, *Nucl. Instrum. Methods Phys. Res., Sect. B* **1999**, *151*, 301.
[15] J. L. Garnett, L. T. Ng, V. Viengkhou, I. W. Hennessy, E. F. Zilic, *Radiat. Phys. Chem.* **2000**, *57*, 355.
[16] J. J. Yu, S. H. Ryu, *J. Appl. Polym. Sci.* **1999**, *73*, 1733.
[17] D. Ruckert, G. Geuskens, *Eur. Polym. J.* **1996**, *32*, 201.
[18] W. T. Yang, B. Rånby, *J. Appl. Polym. Sci.* **1996**, *62*, 545.
[19] B. Mattson, B. Stenberg, *J. Appl. Polym. Sci.* **1993**, *50*, 1247.
[20] H. Kubota, I. G. Suka, S. Kuroda, T. Kondo, *Eur. Polym. J.* **2001**, *37*, 1367.
[21] G. S. Irwan, S. Kuroda, H. Kubota, T. Kondo, *J. Appl. Polym. Sci.* **2002**, *83*, 2454.
[22] H. M. Ma, R. H. Davis, C. N. Bowman, *Macromolecules* **2000**, *33*, 331.
[23] C. Decker, K. Zahouily, *Macromol. Symp.* **1998**, *129*, 99.
[24] T. Wang, E. T. Kang, K. G. Neoh, K. L. Tan, D. J. Liaw, *Langmuir* **1998**, *14*, 921.
[25] T. Kondo, M. Koyama, H. Kubota, R. Katakai, *J. Appl. Polym. Sci.* **1998**, *67*, 2057.
[26] M. Imaizumi, H. Kubota, Y. Hata, *Eur. Polym. J.* **1994**, *30*, 979.
[27] J. P. Deng, W. T. Yang, B. Rånby, *Macromol. Rapid Commun.* **2001**, *22*, 535.
[28] J. P. Deng, W. T. Yang, *J. Polym. Sci., Part A: Polym. Chem.* **2001**, *39*, 3246.
[29] J. F. Moulder, W. F. Stickle, P. E. Sobol, K. B. Bomben, *Handbook of X-ray Photoelectron Spectroscopy* (Eds: J. Chastain, R. C. King Jr.), Physical Electronics, Inc., Eden Prairie, MN **1995**.
[30] I. H. Hagestam, T. C. Pinkerton, *Anal. Chem.* **1985**, *57*, 1757.
[31] J. Haginaka, *TrAC, Trends Anal. Chem.* **1991**, *10*, 17.
[32] C. R. Tewell, F. Malizia, J. W. Ager, G. A. Somorjai, *J. Phys. Chem. B* **2002**, *106*, 2946.